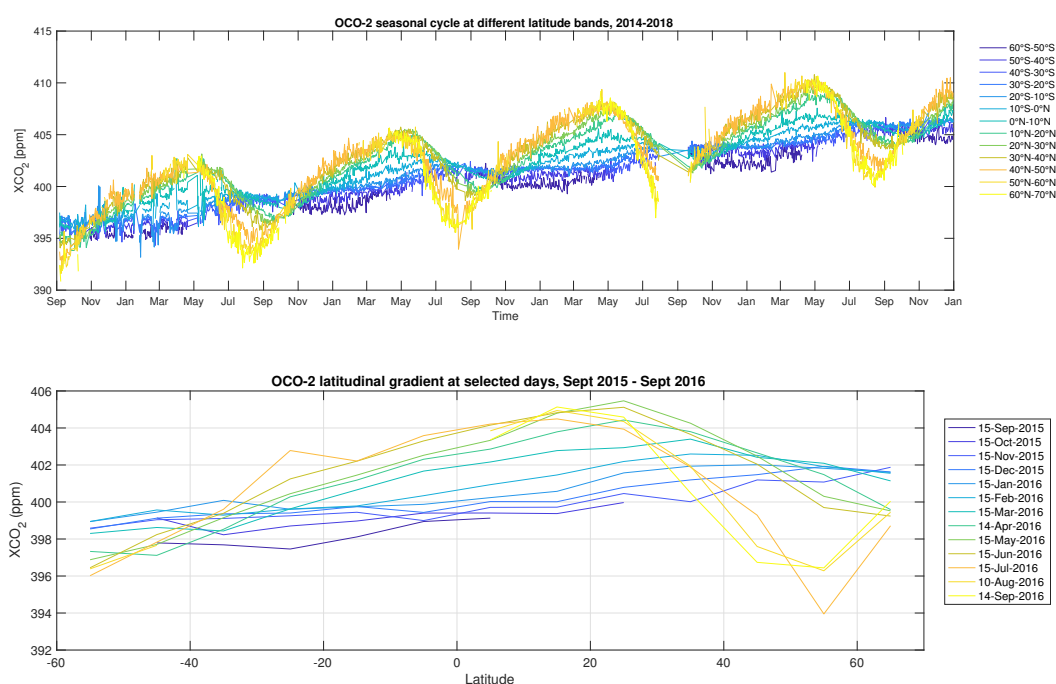


Article

# Supplementary Materials: Analysis of Four Years of Global XCO<sub>2</sub> Anomalies as Seen by Orbiting Carbon Observatory-2

Janne Hakkarainen <sup>1,\*</sup> , Iolanda Ialongo <sup>1</sup> , Shamil Maksyutov <sup>2</sup>  and David Crisp <sup>3</sup> 

Received: 27 February 2019 ; Accepted: 4 April 2019 ; Published: 9 April 2019



**Figure 1.** OCO-2 seasonal cycle at 10 degree latitude bands (top panel) and latitudinal gradient at selected days between September 2015 and September 2016 (bottom panel). See Fig. 2 for daily background.

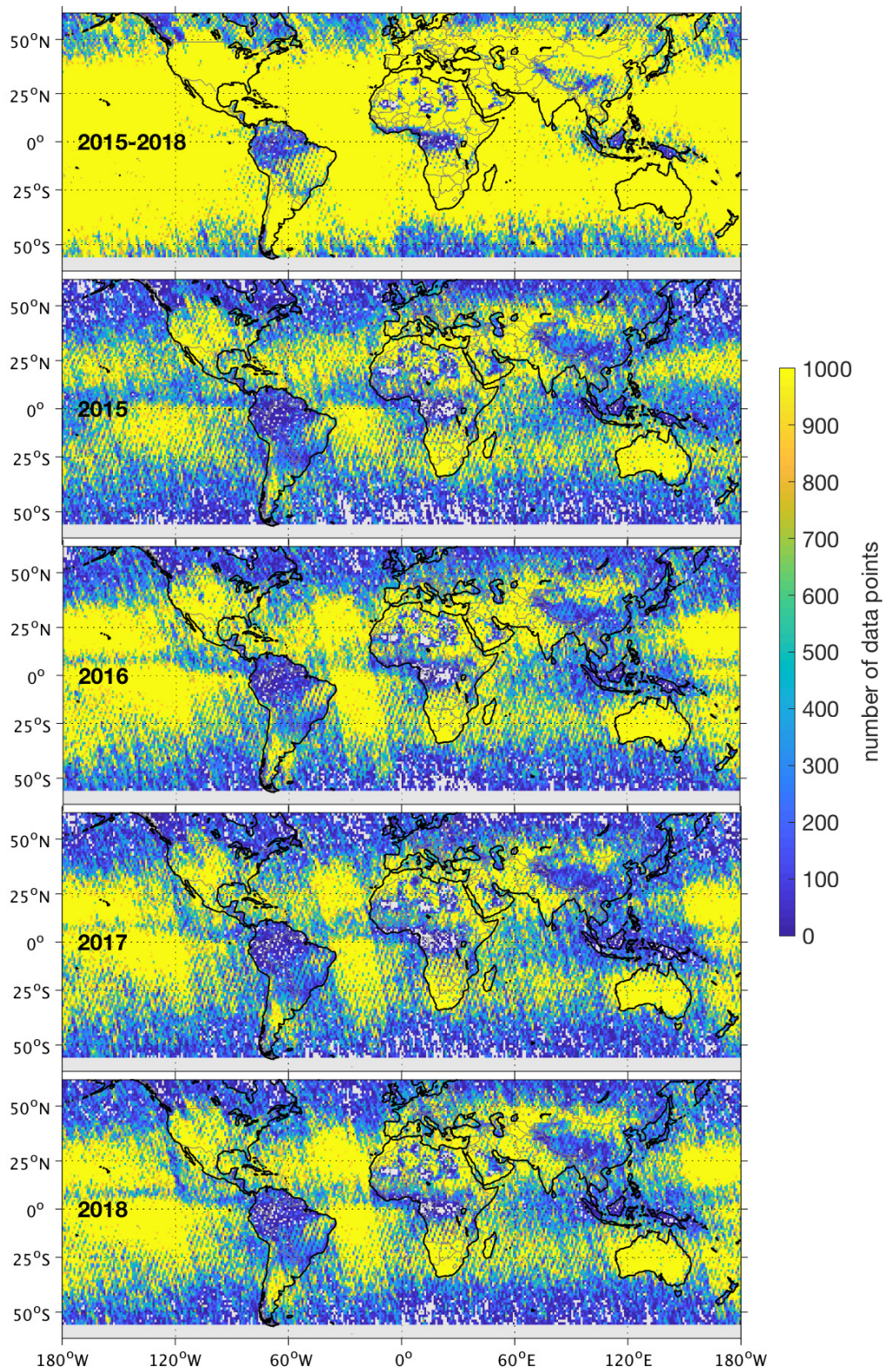


Figure 2. Number of data points on each 1° × 1° grid cell.



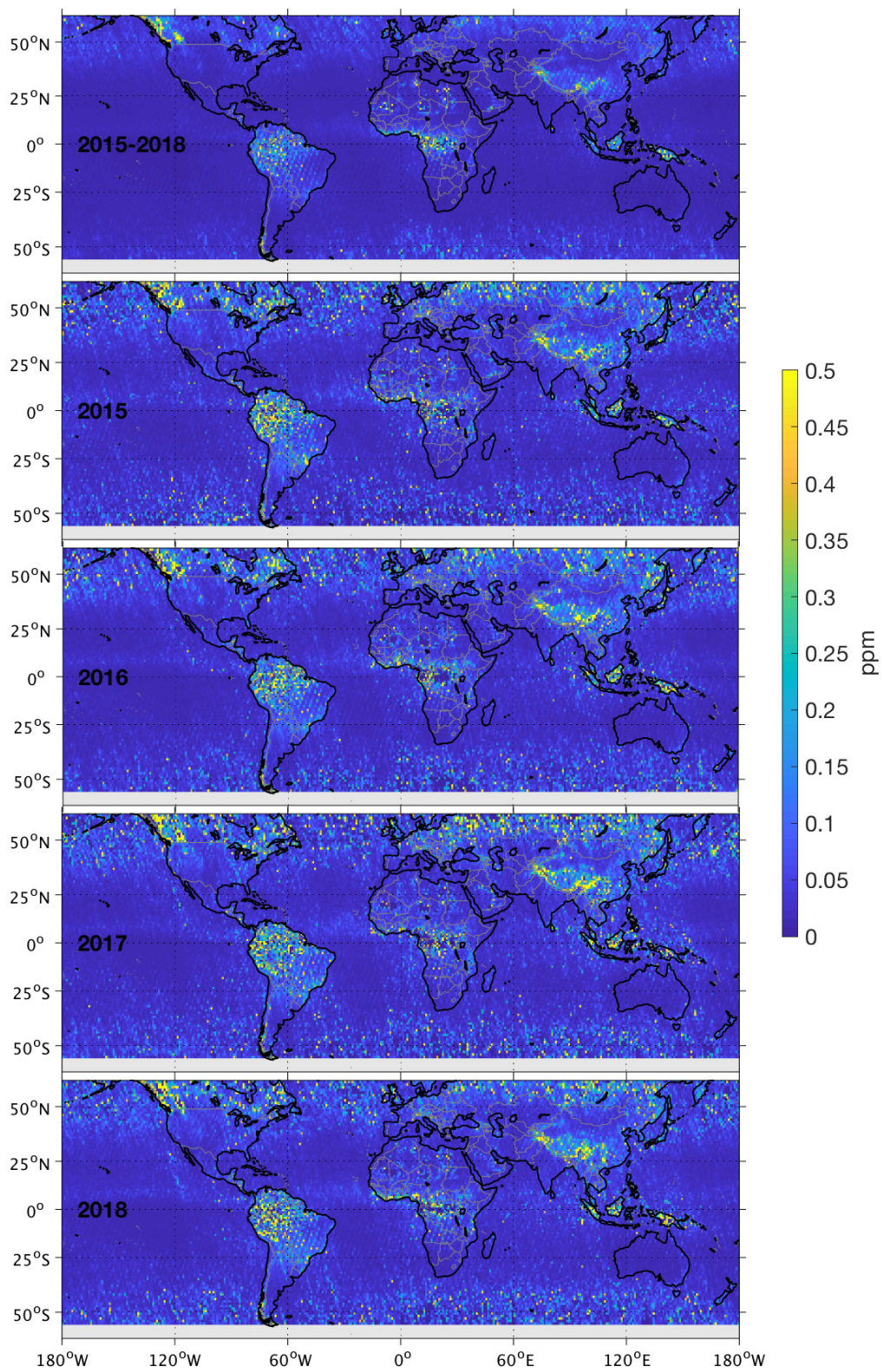
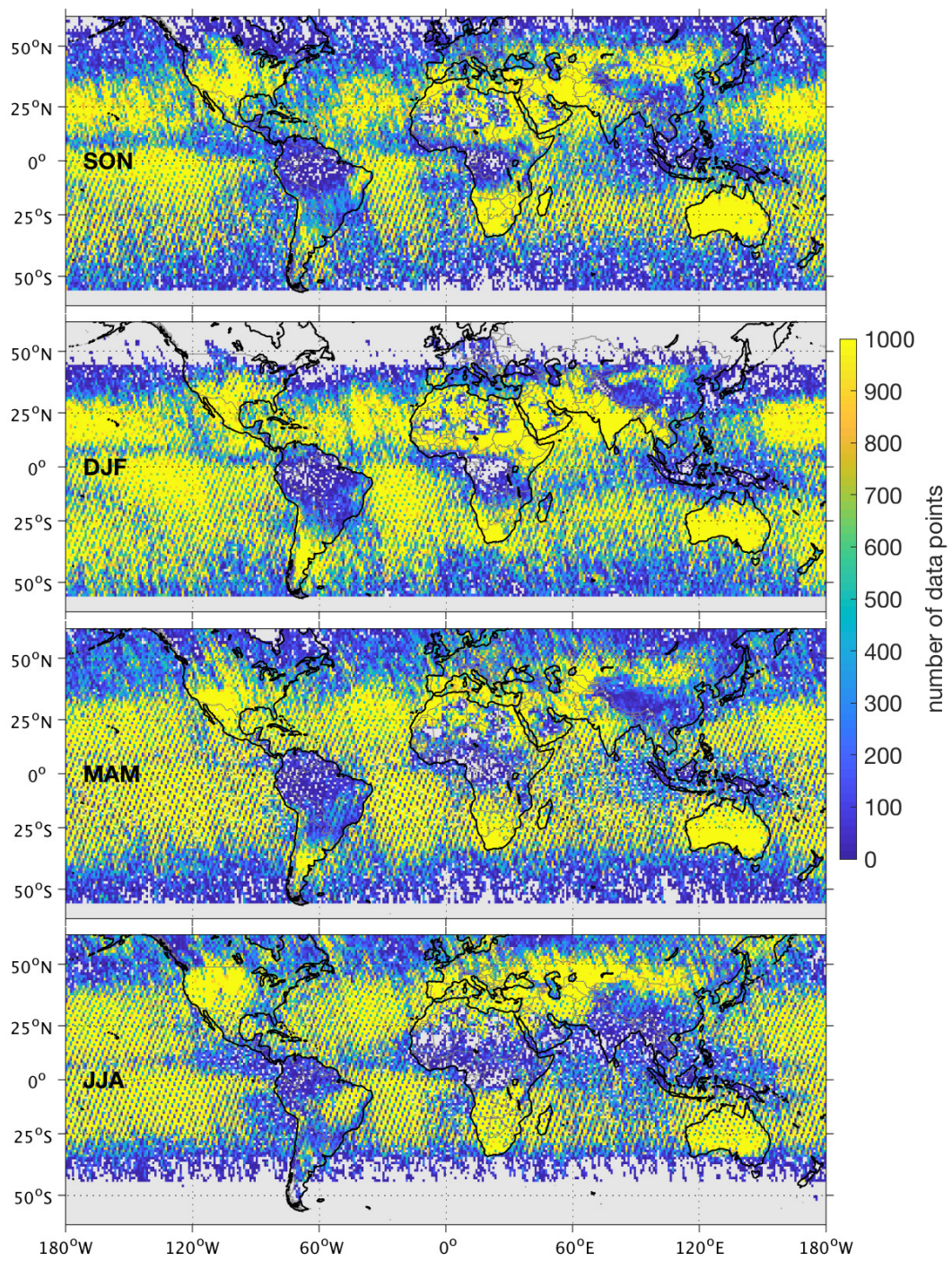


Figure 3. Standard error of the mean on each  $1^\circ \times 1^\circ$  grid cell.





**Figure 4.** Number of data points on each  $1^\circ \times 1^\circ$  grid cell at each season from September 2014 to August 2018.



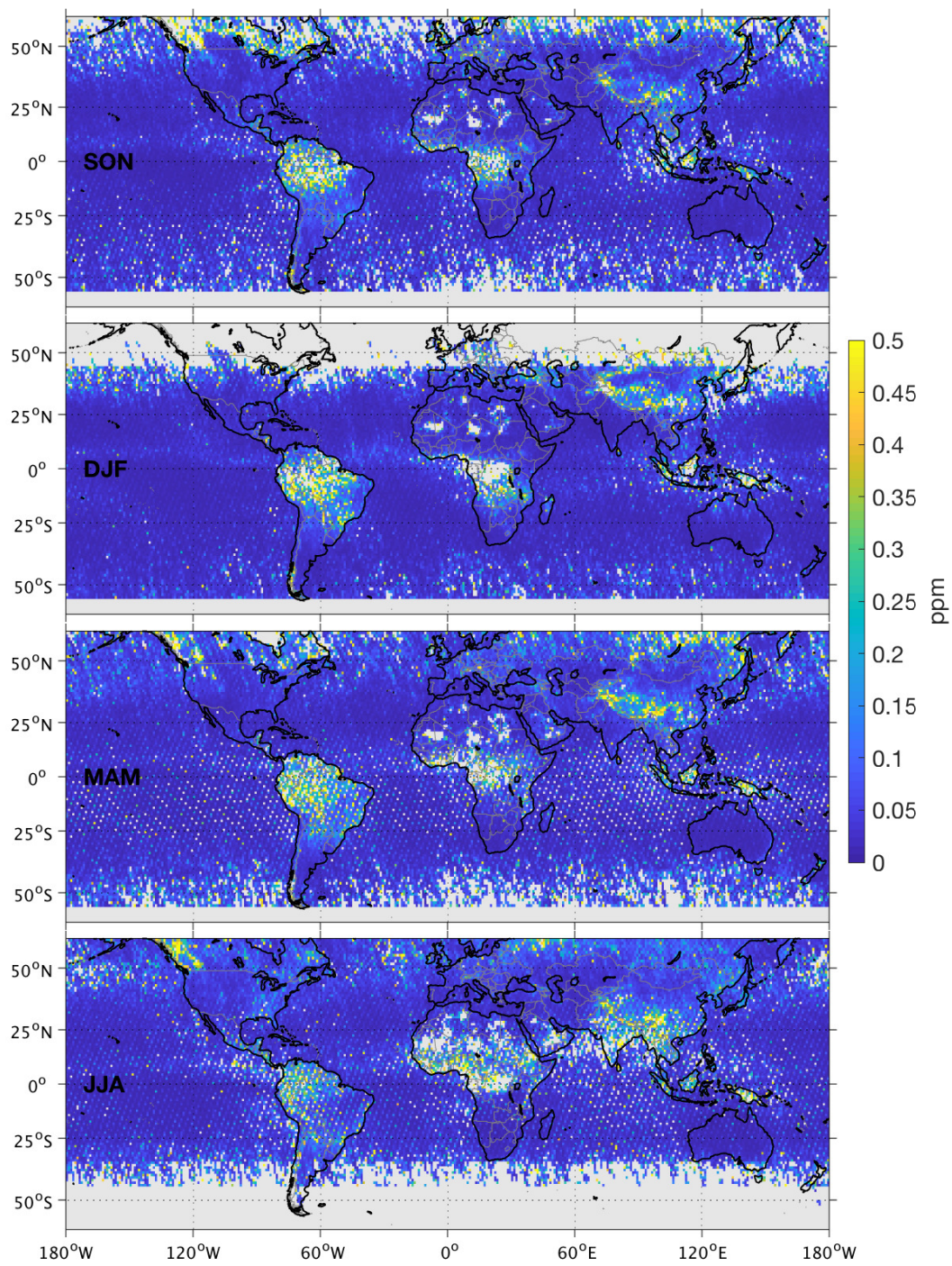
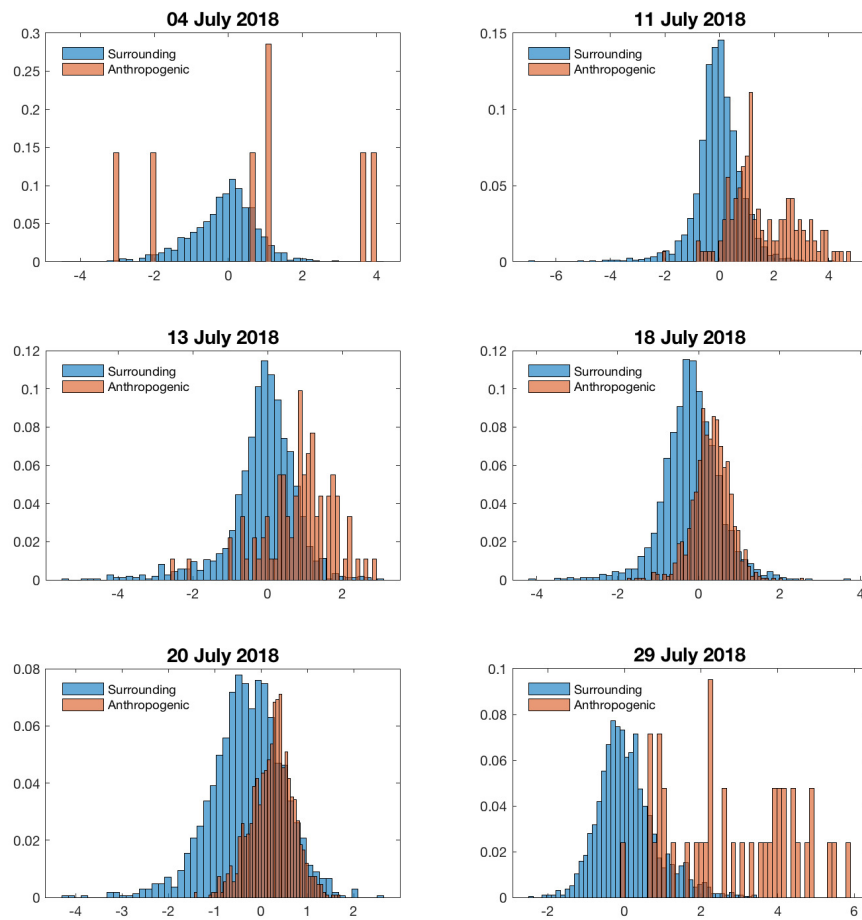


Figure 5. Standard error of the mean for the seasonal XCO<sub>2</sub> anomalies 2014–2018.



**Figure 6.** Histograms of XCO<sub>2</sub> anomalies inside and outside the NO<sub>2</sub> plumes. The anthropogenic and surrounding categories are discriminated according to the collocated tropospheric NO<sub>2</sub> column values (larger or smaller than  $5 \times 10^{15}$  molec./cm<sup>2</sup>, respectively).



© 2019 by the authors. Licensee MDPI, Basel, Switzerland. This article is an open access article distributed under the terms and conditions of the Creative Commons Attribution (CC BY) license (<http://creativecommons.org/licenses/by/4.0/>).